ASTRONOMY & ASTROPHYSICS
SUPPLEMENT SERIES

Astron. Astrophys. Suppl. Ser. **102,** 381-387 (1993)

Optical counterpart of galactic plane variable radio sources

J.M. Paredes[1,2], J. Martí[1], C. Jordi[1,2], E. Trullols[1,3] and M. Peracaula[1]

[1] Departament d'Astronomia i Meteorologia, Universitat de Barcelona, Av. Diagonal 647, E-08028 Barcelona, Spain
[2] Laboratori d'Astrofísica, Societat Catalana de Física (IEC), Spain
[3] Departament de Matemàtica i Telemàtica, Universitat Politècnica de Catalunya, Av. Victor Balaguer s/n, E-08800 Vilanova i la Geltrú, Barcelona, Spain

Received January 28; accepted March 27, 1993

Abstract. — We present *I*-band deep CCD exposures of the fields of galactic plane radio variables. An optical counterpart, based on positional coincidence, has been found for 15 of the 27 observed program objects. The Johnson *I* magnitude of the sources identified is in the range 18-21.

Key words: radio continuum: general — astrometry — techniques: image processing

1. Introduction

The "GT" catalogue was produced as a result of the galactic plane 6 cm radio survey carried out by Gregory & Taylor (1981, 1986) and Taylor & Gregory (1983). It contains up to 1274 discrete radio sources located within galactic coordinates $-2° \leq b \leq 2°$ and $40° \leq l \leq 220°$. One of the goals of its authors was to search for time variable galactic radio sources, whose nature might be similar to that of the peculiar radio emitting X-ray binaries Cyg X-3 and SS 433. Among the objects found, there are at least 28 sources with evidence for short term (few days) and/or long term (few years) time variability, with 6 cm emission levels ranging from tens of mJy to a few Jy (Duric & Gregory, 1988). Their radio morphologies vary from angular sizes less than 0.″1, so unresolved by the VLA, to extended objects with double or triple structure.

A considerable proportion of GT variables are probably extragalactic objects, as suggested by HI absorption observations towards a few objects (Taylor & Seaquist 1984). However, the possibility that some of them are associated to galactic stellar systems cannot be ruled out.

The radio variable GT0236+610 turned out to be coincident with the periodic radio star LSI+61°303 (Taylor & Gregory 1982, 1984). For the remaining GT radio variables, it was not possible to find out their optical counterpart (Duric & Gregory 1988) up to the plate limiting magnitude of the Palomar Observatory Sky Survey (POSS). This is understandable because of the low galactic latitude of these objects, which implies a high degree of extinction along the line of sight. On the other hand, the lack of optical counterpart prevents us from determining directly the galactic or extragalactic nature of a GT variable by looking at its optical spectrum.

As a first step towards solving this problem, the optical counterparts of GT variables must be identified. This task is feasible because the positions of GT variables are known with arcsecond accuracy thanks to the VLA observations in A configuration reported by Duric & Gregory (1988). Previous infrared observations (Elias et al. 1985; Margon et al. 1992) led to the detection of infrared counterparts to the variables GT0116+622, GT0236+610 and GT2100+468.

In this paper, we present the results of an *I*-band CCD identification program for all GT variables listed in Duric & Gregory (1988), except GT0236+610. The identifications were made on the basis of coincidence of optical and radio coordinates within positional error.

2. Observations

The CCD observations were carried out at Calar Alto (Almería, Spain) with the 2.2 m telescope of the Centro Astrónomico Hispano-Alemán (C.A.H.A.), between 21 and 25 October 1992. The Ritchey-Chrétien focus of the telescope was used together with TEK#6 chip. This provides a scale factor of 0.″28 per pixel and a 4.′8 × 4.′8 field of view. In order to minimize galactic plane extinction, the images were obtained through the *I* Johnson filter. This filter has a 900 nm central wavelength and a 100 nm bandpass width. The chip quantum efficiency is 31%.

Exposure times were typically 1800 seconds, yielding limiting I magnitudes of ~ 22. For some prioritary objects, two 1800 second frames were taken and co-added to increase sensitivity. Priority was given to the GT variables with short term variability and VLA compactness. This means that, if they were galactic, they could be excellent candidates to be galactic binaries of the Cyg X-3 type.

Figure 1 shows the CCD fields of our GT program objects. The frames have been treated using standard CCD techniques (bias and dark subtraction and flat-field correction) based on ESO's image processing system MIDAS.

3. Analysis

3.1. *Astrometry and identification procedure*

Primary reference stars were taken from the Guide Star Catalogue (GSC) for the Hubble Space Telescope (Taff et al. 1990; Russell et al. 1990), which is based on the standard epoch J2000.0. However, due to long exposure times and the size of the field of view, fainter reference stars had to be chosen. About ten secondary anonymous stars were considered in each frame and their coordinates were measured on POSS plates using GSC stars as primary reference. The XY coordinates in pixels for these secondary stars were determined using the MIDAS task *center/gauss*. Finally, and astrometric solution for the CCD frame was established. Typically, the residuals of the primary fit were $\lesssim 1''$, while those of the secondary fit were usually smaller, less than $\sim 0''.4$. For each coordinate, the total resulting error of the optical position of an object on a CCD frame can be evaluated following Fugmann et al. (1988) according to:

$$\sigma_{\rm opt} = \left[\left(\sigma_{\rm GSC}^2 + \sigma_1^2\right)/n_1 + \sigma_2^2/n_2 + \sigma_{\rm ref}^2 + \sigma_{\rm CCD}^2\right]^{1/2}, \quad (1)$$

where $\sigma_{\rm GSC}$ is the GSC position error ($\sim 0''.5$), $\sigma_{1,2}$ and $n_{1,2}$ are the respective computed residual rms deviations and degrees of freedom of the primary and secondary fits, $\sigma_{\rm ref}$ represents the relative error between coordinate measurements of bright primary and faint secondary reference stars on POSS plates ($\sim 0''.2$), and $\sigma_{\rm CCD}$ is the error in the coordinate measurement of an optical candidate on the CCD plate (usually negligible).

If there is an object at an optical position $(\alpha_{\rm opt}, \delta_{\rm opt})$ near the radio position $(\alpha_{\rm rad}, \delta_{\rm rad})$, the criterion for considering it a likely optical counterpart is that its normalized distance R should be less than 3, that is:

$$R = \left[\left(\frac{\alpha_{\rm opt} - \alpha_{\rm rad}}{\sigma_\alpha}\right)^2 + \left(\frac{\delta_{\rm opt} - \delta_{\rm rad}}{\sigma_\delta}\right)^2\right]^{1/2} < 3, \quad (2)$$

where σ_α and σ_δ are the combined optical-radio position uncertainty $\sigma = \left(\sigma_{\rm opt}^2 + \sigma_{\rm rad}^2\right)^{1/2}$ in right ascension and declination respectively. For $\sigma_{\rm rad}$ we have taken $\sim 0''.4$, which normaly leads to a total combined uncertainty of $\sim 1''$.

The radio coordinates of the GT variables listed in Duric & Gregory (1988) were converted from B1950.0 to J2000.0 standard epochs following Aoki et al. (1983).

3.2. *Photometry*

The Johnson I magnitude of the optical counterparts was roughly estimated by differential photometry using nearby comparison stars. The comparison stars were taken from the lists of Rosselló et al. (1988), Figueras et al. (1990) and Landolt (1983). On the CCD frames, the count rates were estimated using the MIDAS task *integrate/star*. Magnitudes of GT optical counterparts, in reference to several comparison stars observed the same night, are consistent within an accuracy of $\sim 0^{\rm m}.2$.

4. Results and discussion

Among the 27 GT radio variables observed, we found 15 optical counterparts (56%) on the basis of positional coincidence. One of these counterparts was previously known in the optical (Margon et al. 1992) and another in the infrared (Elias et al. 1985). The 60% of the optical counterpart identified correspond to both compact and short term radio variable objects. In addition, all the optical counterparts detected for objects with triple radio morphology coincide with the central compact component. The presence of a central object, which seems to be powering the radio lobes, is reminiscent of extragalactic radio sources. However, similar morphologies are also observed in well known galactic X-ray binaries, like Cyg X-3 at subarcsec level (Molnar et al. 1988), SS433 at arcsec level (Hjellming & Johnston 1981), and probably up to the arcmin level in the case of 1E1740.9−2942 and GRS1758−258 (Mirabel et al. 1992; Rodríguez et al. 1992).

The results are presented in Fig. 1 and in Table 1. For the 27 objects shown in Fig. 1, the radio position is indicated by a cross, generally near the CCD image center. North is at the top and east to the left. The field shown covers about $70'' \times 70''$ except that corresponding to GT0629+103 which, because it is a very scarce field, measures about $140'' \times 140''$.

First column in Table 1 gives the objet name, while Col. 2 shows the radio morphology and radio variability type from Duric & Gregory (1988). Following these authors, radio morphology is coded as: C for VLA unresolved point sources, CE for a compact core with a faint extension, T for triple sources, TJ for a triple with a jet connecting the core with one or both lobes, D for two components with extended emission, DJ for a double source with a jet, and X for extended complex sources with central core missing. Radio variability type is given as: SV for short-term, LV for long-term, PSV for possible

short-term, and PLV for possible long-term. Columns 3 and 4 give the J2000.0 coordinates of the radio position. When an optical identification was possible ($R < 3$), the Cols. 5 and 6 show the offsets between the optical and radio position and Col. 7 gives the Johnson I magnitude. In the case of no detection a lower limit for the magnitude is given. Finally, Col. 8 gives further remarks.

Some comments on several particular sources follow:

GT0026+627: this radio variable has a double component radio morphology (Duric et al. 1987). The optical counterpart found, which falls near the southern component of the double, is closer than the POSS object proposed by Duric et al. (1987).

GT0034+626: in the radio map of Duric & Gregory (1988) this source presents an elbow-shaped structure with three main components. The optical counterpart detected is coincident with the middle one.

GT0106+613: Gregory & Taylor (1981) found two faint optical objects close to the radio coordinates on POSS plates. We propose as the optical counterpart the faintest of them, which is located $\sim 1\farcs2$ away from the radio position. The other candidate is about two magnitudes brighter but, clearly, it does not satisfy the identification criterion of Eq. (2). In the infrared, at 2.2 μm (K band), Elias et al. (1985) did not detect infrared emission from the position of GT0106+613 up to a limit of 0.9 mJy.

GT0116+622: this radio variable is believed to be associated with the γ-ray source Cas γ-1 (Gregory et al. 1986). Its optical and near infrared counterpart was identified by Margon et al. (1992). We confirm the detection, in the Johnson I band, of a faint object with roughly similar offsets from the radio position. Due to bad weather during the first night of observation, no reliable magnitude could be derived from our CCD image.

GT0255+574: the closest optical object lies $\sim 5''$ to the west.

GT0304+575: in the radio, this source displays a prominent central core with jet lobe structure (Duric & Gregory 1988). Our optical counterpart coincides with this central component.

GT0459+415: optical counterpart found. Not detected by Elias et al. (1985).

GT0506+398: an optical counterpart was found for this object with $I = 20\fm0$. In addition, infrared observations with the *Multi Mirror Telescope* (MMT) at 10 μm place a lower limit magnitude of $N > 8.2$.

GT0554+242: optical counterpart found. Undetected by Elias et al. (1985).

GT0556+239: no optical counterpart found. MMT observations indicate $N > 9.0$.

GT1943+228: an optical object was present at $\sim 3''$ north, but because $R \simeq 5$ we did not consider it the optical counterpart. Moreover, due to the north-south elongated radio morphology (Duric et al. 1987), this object appears to be $\sim 1\farcs5$ away from the northern component.

GT2100+468: Elias et al. (1985) give the infrared photometry of this GT radio variable. They point out that its infrared colors resemble those of Cygnus X-3. However, our CCD plate shows that these findings could be affected by the presence of several background objects inside their beam aperture.

GT2134+536: in this case two optical objects appear near the radio position, at $1\farcs5$ and $1\farcs9$ approximately. Only the closest and faintest one satisfies the identification criterion with $R = 2.9$. Undetected by Elias et al. (1985).

GT2156+531: the optical counterpart coincides with the central component of the triple structure present on the 20 cm map of Taylor et al. (1984). Not detected by Elias et al. (1985).

GT2157+566: this GT variable has associated three different radio source components (Duric et al. 1987). Their location on the corresponding CCD frame of Fig. 1 is marked by crosses labeled A, B and C. The position A coincides with the westernmost radio component. It has three optical objects at $\sim 3''$, but none satisfies the identification criterion. The southern, unresolved radio component C presents a collimated radio structure pointing towards A. No optical objects is seen near C position. Finally, as Duric et al. (1987) point out, the northern component B is probably an unrelated radio source. They also suggest, as possible optical counterpart, two bright POSS stars at $\sim 3''$ from B. However, we have found that the optical counterpart is more likely to be a fainter ($I = 18\fm2$) object present at only $\sim 1\farcs3$ from B.

GT2203+559: this is another example of coincidence between the optical counterpart and the central unresolved core of the triple radio structure detected at 20 cm by Duric et al. (1987). Not detected by Elias et al. (1985).

Acknowledgements. We are grateful the CAHA staff, specially A. Aguirre and M. Alises, for their support in carrying out these observations. We also thank F. Comerón and G.H. Rieke for their infrared observations with the MMT. This work has been partially supported by DGCICYT under contract PB91-0857 and the "Ayudas para la utilización de recursos cientificos"and CICYT under contract ESP93-1020-E. M.P. acknowledges financial support from the Spanish Ministerio de Educación y Ciencia.

References

Aoki S., Sôma M., Kinoshita H., Inoue K. 1983, A&A 128, 263

Duric N., Gregory P.C., Taylor A.R. 1987, AJ 93, 890

Duric N., Gregory P.C. 1988, AJ 95, 1149

Elias J.H., Matthews K., Neugebauer G., Soifer B.T. 1985, AJ 90, 1188

Figueras F., Jordi C., Rosselló G., Torra J. 1990, A&ASS 82, 57

Fugmann W., Meisenheimer K., Röser H.-J. 1988, A&ASS 75, 173

Gregory P.C., Duric N., Reid A., Picha J., Stevenson T., Taylor A.R. 1986, Nat 323, 602
Gregory P.C., Taylor A.R. 1981, ApJ 248, 596
Gregory P.C., Taylor A.R. 1986, AJ 92, 371
Hjellming R.M., Johnston K.J. 1981, Nat 358, 215
Landolt A.U. 1983, AJ 88, 439
Mirabel I.F., Rodríguez L.F., Cordier B., Paul J., Lebrun F. 1992, Nat 358, 215
Molnar L.A., Reid M.J., Grindlay J.E. 1988, ApJ 331, 494
Margon B., Phillips A.C., Ciardullo R., Jacoby H.H. 1992, AJ 103, 924
Rodríguez L.F., Mirabel I.F., Martí J. 1992, ApJ 401, L15
Rosselló G., Figueras F., Jordi C., Núñez J. Paredes J.M., Sala F., Torra J. 1988, A&ASS 75, 21
Russell J.L., Lasker B.M., McLean B.J., Sturch C.R., Jenkner H. 1990, AJ 99, 2059
Taff L.G., Lattanzi M.C., Bucciarelli B., Gilmozzi R., McLean B.J., Jenkner H., Laidler V.G., Lasker B.M., Shara M.M., Sturch C.R. 1990, ApJ 353, L45
Taylor A.R., Gregory P.C. 1982, ApJ 255, 210
Taylor A.R., Gregory P.C. 1983, AJ 88, 1784
Taylor A.R., Gregory P.C. 1984, ApJ 283, 273
Taylor A.R., Seaquist E.R. 1984, AJ 89, 1692
Taylor A.R., Seaquist E.R., Gregory P.C. 1984, AJ 89, 1180
Vermeulen R.C., Schilizzi R.T., Icke V., Fejes I., Spencer R.E. 1987, Nat 328, 309

Table 1. Optical identification of GT radio variables

Object	Radio morphology and variability code[a]	α_{rad} J2000.0	δ_{rad} J2000.0	$(\alpha_{opt}-\alpha_{rad})^b$	$(\delta_{opt}-\delta_{rad})^b$	Johnson I magnitude	Comments
GT0026+627	D SV	$00^h29^m23\overset{s}{.}41$	+63°03′34″.7	+1″.7	+0″.2	20.2	Rev. ident.
GT0034+626	X LV	$00^h37^m11\overset{s}{.}42$	+62°54′38″.5	+0″.1	+0″.2	20.6	New ident.
GT0049+615	CE SV,PLV	$00^h52^m57\overset{s}{.}23$	+61°45′51″.0			>22	Empty field
GT0106+613	C SV,LV	$01^h09^m46\overset{s}{.}35$	+61°33′30″.3	−0″.1	−1″.2	19.4	Revised ident.
GT0116+622	C SV,LV	$01^h19^m17\overset{s}{.}44$	+62°29′15″.3	−1″.3	−0″.5		Confirmation
GT0232+589	CE PSV	$02^h36^m11\overset{s}{.}16$	+59°11′15″.3			>21	Empty field
GT0252+574	C LV	$02^h56^m29\overset{s}{.}06$	+57°36′42″.9			>22	Empty field
GT0255+574	C LV	$02^h59^m39\overset{s}{.}50$	+57°39′12″.7			>21	Empty field
GT0304+575	TJ LV	$03^h08^m09\overset{s}{.}93$	+57°41′57″.3	+0″.5	+0″.1	20.6	New ident.
GT0314+565	C SV,LV	$03^h17^m54\overset{s}{.}93$	+56°43′57″.7			>21	Empty field
GT0342+538	C SV,LV	$03^h46^m34\overset{s}{.}53$	+54°00′59″.3	+1″.2	+0″.6	21.3	New ident.
GT0455+421	C SV	$04^h59^m04\overset{s}{.}40$	+42°08′54″.6	+0″.3	+0″.6	20.4	New ident.
GT0459+415	C SV,LV	$05^h02^m38\overset{s}{.}00$	+41°39′19″.2	+1″.2	−0″.3	18.6	New ident.
GT0506+398	C SV,PLV	$05^h09^m48\overset{s}{.}82$	+39°51′54″.5	−0″.6	−0″.2	20.0	New ident.
GT0554+242	C SV,LV	$05^h57^m04\overset{s}{.}72$	+24°13′55″.2	+0″.8	+0″.2	18.8	New ident.
GT0556+239	C SV,LV	$05^h59^m32\overset{s}{.}04$	+23°53′53″.8			>22	Empty field
GT0629+103	C SV	$06^h32^m15\overset{s}{.}34$	+10°22′02″.0			>21	Empty field
GT0630+082	D SV,LV	$06^h33^m13\overset{s}{.}00$	+08°13′18″.7			>21	Empty field
GT1937+215	X PSV,LV	$19^h39^m39\overset{s}{.}33$	+21°37′33″.4	+0″.4	+0″.9	17.8	New ident.
GT1943+228	CE PSV,LV	$19^h46^m06\overset{s}{.}26$	+23°00′04″.3			>22	Empty field
GT2100+468	C SV,LV	$21^h02^m17\overset{s}{.}06$	+47°02′16″.1	+0″.7	+0″.6	21.3	IR source
GT2134+536	C SV	$21^h36^m19\overset{s}{.}23$	+53°52′15″.6	−1″.5	+0″.1	18.8	New ident.
GT2156+531	TJ PSV	$21^h57^m48\overset{s}{.}85$	+53°23′32″.5	+0″.4	+0″.2	20.8	New ident.
GT2157+566	TJ SV	$21^h59^m34\overset{s}{.}33$	+56°56′17″.0			>22	Empty field[c]
GT2203+559	T PSV	$22^h05^m28\overset{s}{.}36$	+56°09′45″.1	−0″.1	+0″.3	21.2	New ident.
GT2241+606	CE PSV	$22^h43^m00\overset{s}{.}86$	+60°55′44″.6			>20	Empty field
GT2257+577	DJ PSV	$23^h00^m03\overset{s}{.}50$	+57°58′23″.9			>22	Empty field

[a] From Duric & Gregory (1988).
[b] Total estimated positional offset error is ±1″.
[c] See comments in the text.

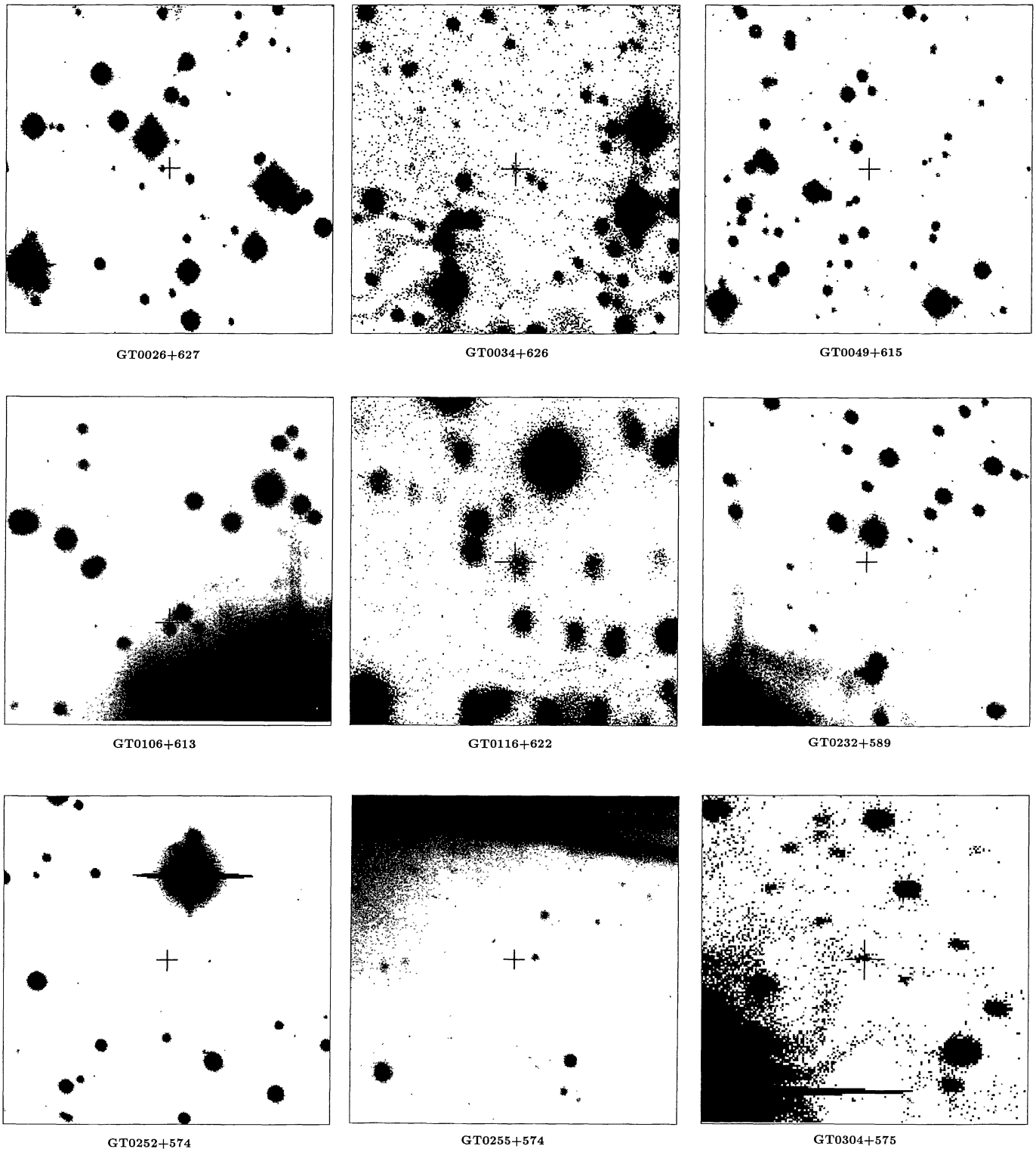

Fig. 1. CCD images in the Johnson *I* band of the field of observed GT radio variables. North is at the top and east to the left. The radio position is shown by a cross. The fields are about $70'' \times 70''$ size except for GT0629+103 which is twice this size. The crosses labeled A, B, and C in the frame of GT2157+566 are identified in the text

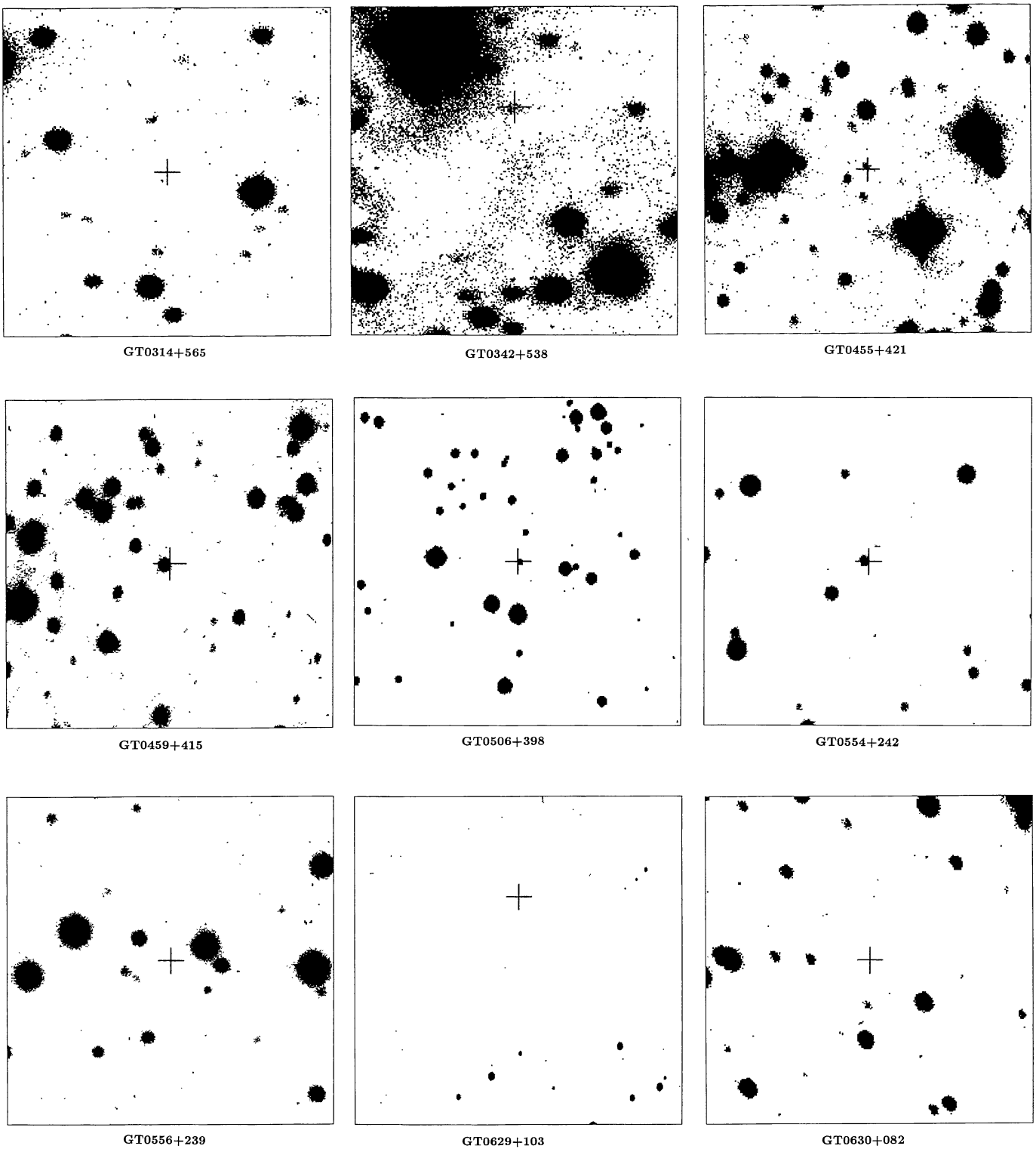

Fig. 1. continued

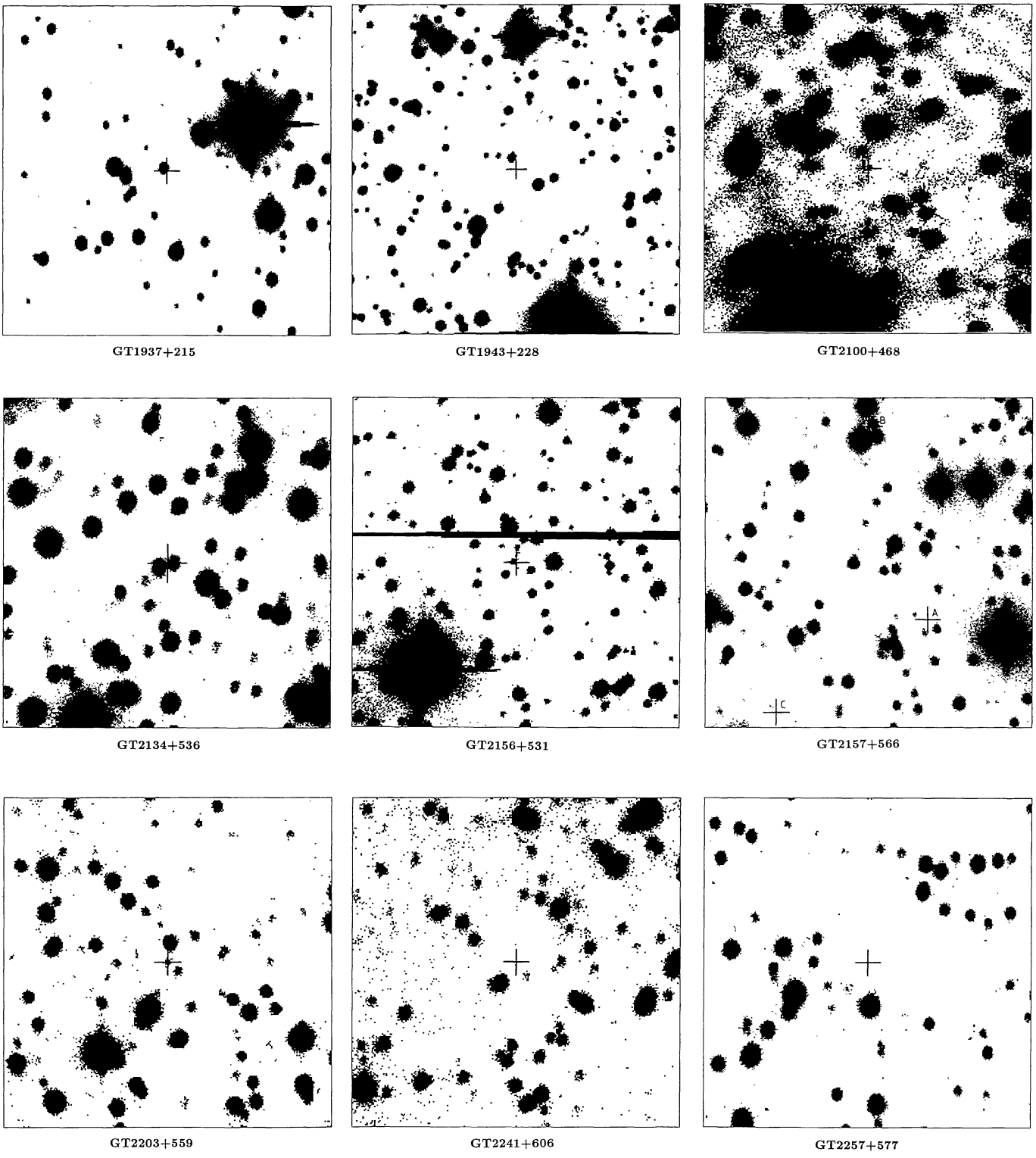

Fig. 1. continued